

Exact Surface States in Photonic Superlattices

Qiongtao Xie^{1,2*} and Chaohong Lee^{2,3†}

¹*Department of Physics and Key Laboratory of Low-Dimensional Quantum Structure and Quantum Control of Ministry of Education, Hunan Normal University, Changsha 410081, China*

²*State Key Laboratory of Optoelectronic Materials and Technologies, School of Physics and Engineering, Sun Yat-Sen University, Guangzhou 510275, China and*

³*Nonlinear Physics Centre, Research School of Physics and Engineering, Australian National University, Canberra ACT 0200, Australia*

(Dated: February 20, 2019)

We develop an analytical method to derive exact surface states in photonic superlattices. In a kind of infinite bichromatic superlattices satisfying some certain conditions, we analytically obtain their in-gap states, which are superpositions of finite numbers of unstable Bloch waves. By using the unstable in-gap states, we construct exactly several stable surface states in various photonic superlattices. We analytically explore the parametric dependence of these exact surface states. Our analysis provides an exact demonstration for the existence of surface states and would be also helpful to understand surface states in other lattice systems.

PACS numbers: 42.25.Gy, 42.70.Qs, 73.20.At

I. INTRODUCTION

Surface states are a kind of localized states found at the interfaces between two different media. In 1932, Tamm predicted that electronic surface waves may exist in a semi-infinite one-dimensional Kronig-Penney (KP) model [1] and these surface states were named as Tamm states later. The energies of Tamm states lie in the forbidden gaps for the corresponding infinite KP model. The surface states depend crucially on surface termination of periodic potentials [2]. It has been demonstrated that Tamm states appear when the periodic potentials are asymmetrically terminated and Shockley states appear while the periodic potentials are symmetrically terminated [2]. Surface states have been observed in several experimental systems such as semiconductor superlattices, magneto-photonic structures and photonic superlattices [3–14].

In the past few decades, surface states have been studied extensively due to their potential applications in optoelectronic devices. However, an analytical demonstration of the existence of exact surface states is still absent [15–26]. For an example, to construct a surface state in the semi-infinite one-dimensional KP model, one need to calculate analytically or numerically a Bloch wave of a complex wave number and then match it with an exponentially decaying state inside the surface potential [15–17]. The Bloch wave of a complex wave number is an unstable in-gap state. Up to now, it is still a great challenge to find exact solutions for unstable in-gap states in superpositions of finite terms.

In this paper, for a kind of infinite bichromatic su-

perlattices satisfying some certain conditions, we analytically find their in-gap states in superpositions of finite numbers of unstable Bloch waves. These unstable in-gap states are then used to exactly construct stable surface states for several typical systems of surface states, such as the semi-infinite photonic superlattice, the finite photonic superlattice, two directly coupled photonic superlattices, and two indirectly coupled photonic superlattices. The conditions for the existence of these exact surface states are derived analytically. We find that the symmetry and the existence of the surface states depend crucially on both lattice parameters and interface parameters. Our analytical results of surface states provide an optional benchmark for understanding surface waves in lattice systems.

II. EXACT IN-GAP STATES IN PHOTONIC SUPERLATTICES

We consider the light propagation in a one-dimensional waveguide array. Assuming the waveguide array is aligned along the X direction and the light is localized along the Y direction, the propagation of the light electric field $E(X, Z)$ along the Z direction is described by an effective two-dimensional wave equation [27],

$$i \frac{\lambda}{2\pi} \frac{\partial E}{\partial Z} = - \frac{\lambda^2}{8\pi^2 n_s} \frac{\partial^2 E}{\partial X^2} + U(X)E, \quad (1)$$

where λ is the free-space light wavelength and n_s is the substrate refractive index. The profile of the effective refractive index is in form of $U(X) = [n_s^2 - n^2(X)]/(2n_s) \simeq n_s - n(X)$ with the refractive index $n(X)$ for the waveguide array. By using the periodic modulation techniques of $n(X)$ [28], one can build a bichromatic superlattice of $U(X) = n_1 [1 - \cos(\frac{2\pi X}{\Lambda})] + n_2 [1 + \cos(\frac{\pi X}{\Lambda} + \theta)]$ with the amplitudes n_1 and n_2 , the modulation period 2Λ and the relative phase θ .

*Electronic address: xieqiongtao@yahoo.cn

†Electronic address: chleecn@gmail.com

By introducing two scaled variables $x = \pi X/\Lambda$ and $z = \pi\lambda Z/(4\Lambda^2 n_s)$ and a transformation $\phi(x, z) = E(x, z) \exp[i(n'_1 + n'_2)z]$ with $n'_1 = 8\Lambda^2 n_s n_1/\lambda^2$ and $n'_2 = 8\Lambda^2 n_s n_2/\lambda^2$, the system is then described by

$$i \frac{\partial \phi}{\partial z} = -\frac{\partial^2 \phi}{\partial x^2} + V(x)\phi, \quad (2)$$

with $V(x) = -n'_1 \cos(2x) + n'_2 \cos(x + \theta)$. Considering its stationary states, $\phi(x, z) = \psi(x) \exp[-i\beta z]$, the amplitude $\psi(x)$ obeys a time-independent equation

$$\beta \psi = -\frac{\partial^2 \psi}{\partial x^2} + V(x)\psi, \quad (3)$$

with β denoting the propagation constant. Obviously, the light propagation is equivalent to a quantum particle in an external potential.

According to Bloch's theorem, the solutions for Eq. (3) can be written in form of $\psi(x) = \exp[ikx]u(x)$, where k is the wave number and $u(x)$ has the same periodicity of $V(x)$. Under condition of $n'_1 = 2\eta^2$, $n'_2 = 2\eta\sqrt{(N+1)^2 + \Delta^2}$ and $\theta = \arctan(\Delta/(N+1))$ with integers $N \geq 0$, $V(x) = V(\eta, \Delta, N, x)$, we find a set of Bloch-wave solutions (see more details in the Appendix),

$$\begin{aligned} \psi_N^{m_1}(\eta, \Delta, x) &= \exp\left[-\left(\frac{\Delta}{2}x + 2\eta \cos x\right)\right] \\ &\times \sum_{n=0}^N \left[a_n \cos\left(\frac{N}{2} - n\right)x - b_n \sin\left(\frac{N}{2} - n\right)x \right], \end{aligned} \quad (4)$$

with a complex wave number $k = N/2 + i\Delta/2$ and a propagation constant $\beta_N^{m_1}$. Here, a_n and b_n can be derived from two recursive series: $2\eta(n+2)a_{n+2} + [(n+1)(n+1-N) + (N^2 + \Delta^2)/4 - 2\eta^2 - \beta_N^{m_1}]a_{n+1} + 2\eta(N-n)a_n + [(n+1)\Delta - N\Delta/2]b_n = 0$ and $2\eta(n+2)b_{n+2} + [(n+1)(n+1-N) + (N^2 + \Delta^2)/4 - 2\eta^2 - \beta_N^{m_1}]b_{n+1} + 2\eta(N-n)b_n + [N\Delta/2 - (n+1)\Delta]a_n = 0$ with initial conditions of $a_0 = 1$, $b_0 = 0$, $a_1 = ((N^2 + \Delta^2)/4 - 2\eta^2 - \beta_N^{m_1})/(2\eta)$ and $b_1 = N\Delta/2$. The propagation constant $\beta_N^{m_1}$ corresponds to the m_1 -th real zeros of $d_{N+1}(\eta, \Delta, \beta) = a_{N+1} + ib_{N+1} = 0$ in ascending order. Since $d_{N+1}(\eta, \Delta, \beta)$ is a polynomial of degree $N+1$ in the propagation constant β , $\beta_N^{m_1}$ have at most $N+1$ solutions. Mathematically, one can construct a linearly independent solution for $\psi_N^{m_1}$ in form of $\tilde{\psi}_N^{m_1} = \psi_N^{m_1} \int_{-\infty}^x (\psi_N^{m_1})^{-2} dx$. Although $\psi_N^{m_1}$ and $\tilde{\psi}_N^{m_1}$ have the same propagation constant $\beta_N^{m_1}$, their divergence properties are opposite: $\psi_N^{m_1} \rightarrow 0$ when $\tilde{\psi}_N^{m_1} \rightarrow \infty$ and vice versa.

In principle, for a given superlattice $V(\eta, \Delta, N, x)$, one may determine the coefficients for the finite-superposition solutions from the two recursive series. For $N \leq 3$, one can easily obtain the exact forms for a_n and b_n . However, if $N > 3$, it is very difficult to give the exact forms for a_n and b_n , and one has to find their values by using numerical methods. Below, we consider the two simplest cases: $N = 0$ and $N = 1$. For the case of $N = 0$,

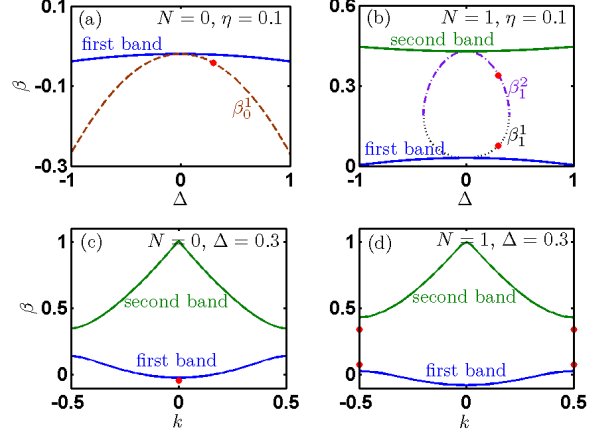


FIG. 1: (Color online). Band-gap structures for $V(\eta, \Delta, N, x)$. (a) The first band at $k = 0$ and the in-gap propagation constant β_0^1 for $N = 0$ and $\eta = 0.1$. (b) The first two bands at $k = \pm 0.5$ and the in-gap propagation constants $\beta_1^{1,2}$ for $N = 1$ and $\eta = 0.1$. (c) The first two bands and β_0^1 for $N = 0$ and $\Delta = 0.3$. (d) The first two bands and $\beta_1^{1,2}$ for $N = 1$ and $\Delta = 0.3$. In which, the red dot in (a) corresponds to the one in (c), and the two red dots in (b) correspond to the four red dots in (d).

the sole finite-superposition solution is expressed as

$$\psi_0^1(\eta, \Delta, x) = \exp\left[-\frac{\Delta}{2}x - 2\eta \cos x\right], \quad (5)$$

with $\beta_0^1(\eta, \Delta) = -(\Delta^2 + 8\eta^2)/4$. For the case of $N = 1$, there are two finite-superposition solutions. The first finite-superposition solution is in form of

$$\begin{aligned} \psi_1^1(\eta, \Delta, x) &= \exp\left[-\frac{\Delta}{2}x - 2\eta \cos x\right] \\ &\times \left[\left(4\eta - \sqrt{16\eta^2 - \Delta^2}\right) \cos\left(\frac{x}{2}\right) - \Delta \sin\left(\frac{x}{2}\right)\right], \end{aligned} \quad (6)$$

with $\beta_1^1(\eta, \Delta) = (1 - \Delta^2 - 8\eta^2 - 2\sqrt{16\eta^2 - \Delta^2})/4$. The other finite-superposition solution reads as

$$\begin{aligned} \psi_1^2(\eta, \Delta, x) &= \exp\left[-\frac{\Delta}{2}x - 2\eta \cos x\right] \\ &\times \left[\left(4\eta + \sqrt{16\eta^2 - \Delta^2}\right) \cos\left(\frac{x}{2}\right) - \Delta \sin\left(\frac{x}{2}\right)\right], \end{aligned} \quad (7)$$

with $\beta_1^2(\eta, \Delta) = (1 - \Delta^2 - 8\eta^2 + 2\sqrt{16\eta^2 - \Delta^2})/4$.

In comparison with the band-gap structure, if $\Delta \neq 0$, we find that β_0^1 falls into the semi-infinite gap below the lowest band and $\beta_1^{1,2}$ lies in the first band-gap, see Fig. 1. This means that these finite-superposition solutions are a kind of in-gap states. If $\Delta = 0$, the finite-superposition solutions become stable Bloch-wave solutions, since the wave numbers become real. Interestingly, β_1^1 and β_1^2 form a closed circle connecting the first two bands at $\Delta = 0$, see Fig. 1(b). Moreover, the in-gap state ψ_0^1 appears

at $k = 0$, while the in-gap states $\psi_1^{1,2}$ appear at $k = \pm 0.5$, see Fig. 1(c) and (d). Since the in-gap states grow without bound, they are unphysical states for the infinite periodic system. However, as we will show below, the in-gap states can be used to construct exact surface states in several typical models.

III. SURFACE STATES IN SINGLE-INTERFACE SYSTEMS

One of the most famous single-interface systems is a semi-infinite periodic system of a truncated $V(\eta, \Delta, N, x)$ connecting a constant refractive index V_0 [1, 3, 8–10, 15–18]. The potential for such a system reads as,

$$V_1(\eta, \Delta, N, x) = \begin{cases} V_0, & x \leq x_0 \text{ (region I)}, \\ V(\eta, \Delta, N, x), & x > x_0 \text{ (region II)}. \end{cases}$$

For an allowed surface state, in the region II, it should be in form of $\psi_N^{m_1}(\eta, \Delta, x)$ for $\Delta > 0$ (or $\tilde{\psi}_N^{m_1}$ for $\Delta < 0$), $\psi_{\text{II}}(x) = C_2 \psi_N^{m_1}$ (or $\psi_{\text{II}}(x) = C_2 \tilde{\psi}_N^{m_1}$). Below we will only consider the case of $\Delta > 0$. In the region I, $\psi_{\text{I}}(x) = C_1 \exp[\sqrt{V_0 - \beta_N^{m_1}} x]$ if $V_0 > \beta_N^{m_1}$. The coefficients C_i are determined by the normalization condition. By applying the continuity condition at the interface $x = x_0$, we find that $\sqrt{V_0 - \beta_N^{m_1}}(\eta, \Delta) = W_N^{m_1}(\eta, \Delta, x_0)$ with $W_N^{m_1}(\eta, \Delta, x) = \dot{\psi}_N^{m_1}(\eta, \Delta, x)/\psi_N^{m_1}(\eta, \Delta, x)$. Here, the dot denotes the derivative with respect to x . Thus the surface state exists if $W_N^{m_1}(\eta, \Delta, N, x_0) > 0$ and $V_0 = \beta_N^{m_1} + (W_N^{m_1})^2$. In Fig. 2(a), we show an exact surface wave in this semi-infinite periodic system with $\eta = 0.3$, $\Delta = 0.2$ and $N = 0$, which corresponds to $n_1 = 2.2 \times 10^{-4}$, $n_2 = 7.6 \times 10^{-4}$ and $\theta = \arctan(0.2)$ in an experimental system of $\lambda = 980$ nm, $n_s = 1.518$ and $\Lambda = 8$ μm [27, 28].

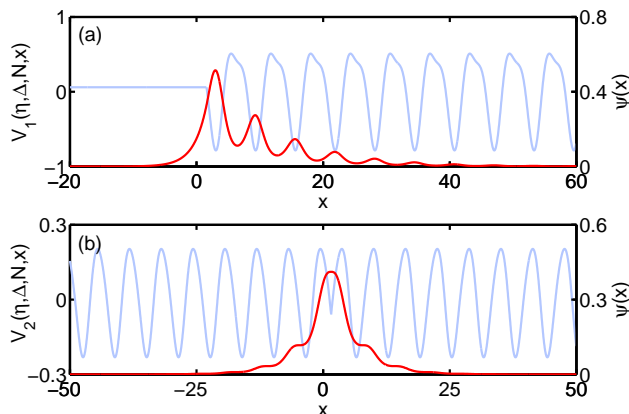


FIG. 2: (Color online). Exact surface states in single-interface systems. (a) $V_1(\eta, \Delta, N, x)$ of $x_0 = \pi/2$, $\eta = 0.3$, $\Delta = 0.2$, $V_0 = 0.12$ and $N = 0$. (b) $V_2(\eta, \Delta, N, x)$ of $x_0 = \pi/2$, $\eta = 0.1$, $\Delta = 4\eta \sin x_0$ and $N = 0$.

Another typical single-interface system is of two truncated periodic potentials connecting at the interface. We

consider a system of $V(-\eta, -\Delta, N, x)$ and $V(\eta, \Delta, N, x)$ with $\Delta > 0$ connecting at the interface $x = x_0$ [11–14, 24]. Its potential is expressed as

$$V_2(\eta, \Delta, N, x) = \begin{cases} V(-\eta, -\Delta, N, x), & x \leq x_0 \text{ (region I)}, \\ V(\eta, \Delta, N, x), & x > x_0 \text{ (region II)}. \end{cases}$$

Thus, we have $\psi_{\text{I}}(x) = C_1 \psi_N^{m_1}(-\eta, -\Delta, x)$ for $x \leq x_0$ and $\psi_{\text{II}}(x) = C_2 \psi_N^{m_1}(\eta, \Delta, x)$ for $x > x_0$. The continuity conditions at $x = x_0$ give $W_N^{m_1}(-\eta, -\Delta, N, x_0) = W_N^{m_1}(\eta, \Delta, N, x_0)$. For the case of $N = 0$, it is easy to find $4\eta \sin x_0 = \Delta$ from the continuity condition at the interface. Therefore, the surface wave exists only when $|\Delta/4\eta| \leq 1$. In Fig. 2(b), we show an exact surface states for $N = 0$ and $x_0 = \pi/2$. We also find that the position of the interface x_0 affects strongly the shape of the surface waves. For an example, the surface wave for the case of $x_0 = \pi/2$ is symmetric about $x = x_0 = \pi/2$. While the surface wave for the case of $x_0 = \pi/6$ is asymmetric about $x = x_0 = \pi/6$.

IV. SURFACE STATES IN DOUBLE-INTERFACE SYSTEMS

One typical double-interface system is a finite periodic system $V(\eta, \Delta, N, x)$ sandwiched by two constant refractive indices V_0 and V_1 [2, 7, 19–23], which obeys the potential

$$V_3(\eta, \Delta, N, x) = \begin{cases} V_0, & x \leq x_0 \text{ (region I)}, \\ V(\eta, \Delta, N, x), & x_0 < x < x_1 \text{ (region II)}, \\ V_1, & x \geq x_1 \text{ (region III)}. \end{cases}$$

In the region II, one may use the finite-superposition solution $\psi_N^{m_1}(\eta, \Delta, x)$ and its linearly independent solution $\tilde{\psi}_N^{m_1}$ to construct the surface state, that is, $\psi_{\text{II}}(x) = C_2 \psi_N^{m_1}(\eta, \Delta, x) + \tilde{C}_2 \tilde{\psi}_N^{m_1}$. In other two regions, the physical state must be non-divergent and normalizable. Therefore, if $V_{0,1} > \beta_N^{m_1}$, we have $\psi_{\text{I}}(x) = C_1 \exp[\sqrt{V_0 - \beta_N^{m_1}} x]$ for $x \leq x_0$ and $\psi_{\text{III}}(x) = C_3 \exp[-\sqrt{V_1 - \beta_N^{m_1}} x]$ for $x \geq x_1$. Similarly, the continuity conditions at the two interfaces $x = x_0$ and $x = x_1$ request

$$\sqrt{V_1 - \beta_N^{m_1}} = -\frac{W_N^{m_1}(\eta, \Delta, x_1) + R \cdot K_N^{m_1}(x_1)}{1 + R \cdot F_N^{m_1}(x_1)}, \quad (8)$$

with

$$R = \tilde{C}_2/C_2 = \frac{\sqrt{V_0 - \beta_N^{m_1}} - W_N^{m_1}(\eta, \Delta, x_0)}{K_N^{m_1}(x_0) - \sqrt{V_0 - \beta_N^{m_1}} F_N^{m_1}(x_0)},$$

$K_N^{m_1}(x) = \tilde{\psi}_N^{m_1}(x)/\psi_N^{m_1}(x)$ and $F_N^{m_1}(x) = \tilde{\psi}_N^{m_1}(x)/\psi_N^{m_1}(x)$. In principle, the ratio between C_2 and \tilde{C}_2 can be arbitrary. However, to satisfy the continuity conditions at the two interfaces, the interface parameters (V_0, V_1, x_0, x_1) and the lattice parameters (η, Δ, N) should obey some certain conditions. In Fig. 3,

we show two surface states for $\eta = 0.3$, $\Delta = 0.1$, $N = 0$ and $x_0 = -x_1 = -19\pi/2$. If $R = 0$, the continuity conditions request $V_0 = 0.12$ and $V_1 = 0.24$ and the surface state is localized around the interface $x = x_0$, see Fig. 3(a). If $R = \infty$ ($C_2 = 0$), the continuity conditions request $V_0 = 0.196151$ and $V_1 = 0.142676$ and the surface state is localized around the interface $x = x_1$, see Fig. 3(b). If $R = 0.0696$, the continuity conditions request $V_0 = 0.123884$ and $V_1 = 0.147421$ and the surface state is almost equally localized around $x = x_0$ and $x = x_1$, see Fig. 3(c).

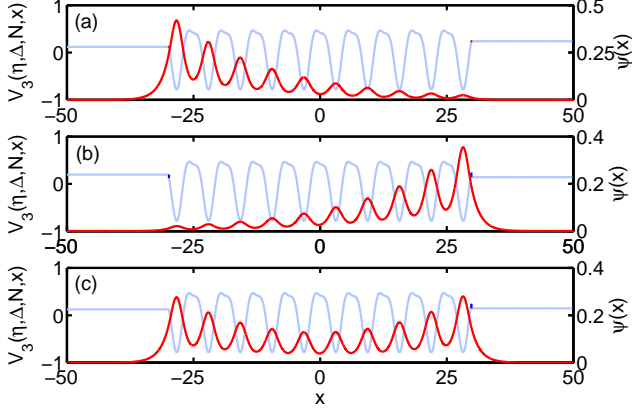


FIG. 3: (Color online). Exact surface states in a finite periodic system described by $V_3(\eta, \Delta, N, x)$ with $N = 0$, $\eta = 0.3$, $\Delta = 0.1$, and $x_0 = -x_1 = -19\pi/2$. (a) $V_0 = 0.12$, $V_1 = 0.24$, and $R = 0$. (b) $V_0 = 0.196151$ and $V_1 = 0.142676$, and $R = \infty$. (c) $V_0 = 0.123884$, $V_1 = 0.147421$, and $R = 0.0696$.

Another typical double-interface system is a constant refractive index V_0 sandwiched by two truncated periodic systems $V(\eta, -\Delta, N, x)$ and $V(\eta, \Delta, N, x)$ [25, 26]. The corresponding refractive index profile is in form of

$$V_4(\eta, \Delta, N, x) = \begin{cases} V(\eta, -\Delta, N, x), & x \leq x_0 \text{ (region I)}, \\ V_0, & x_0 < x < x_1 \text{ (region II)}, \\ V(\eta, \Delta, N, x), & x \geq x_1 \text{ (region III)}. \end{cases}$$

Thus, we have $\psi_I(x) = C_1 \psi_N^{m_1}(\eta, -\Delta, x)$ in the region I, $\psi_{II}(x) = C_2^- \exp[-\sqrt{V_0 - \beta_N^{m_1}} x] + C_2^+ \exp[+\sqrt{V_0 - \beta_N^{m_1}} x]$ in the region II, and $\psi_{III}(x) = C_3 \psi_N^{m_1}(\eta, \Delta, x)$ in the region III. The continuity conditions request

$$\frac{W_N^{m_1}(\eta, \Delta, x_1)}{\sqrt{V_0 - \beta_N^{m_1}}} = \frac{R \cdot \exp[2\sqrt{V_0 - \beta_N^{m_1}} x_1] - 1}{R \cdot \exp[2\sqrt{V_0 - \beta_N^{m_1}} x_1] + 1}, \quad (9)$$

with

$$R = \frac{C_2^+}{C_2^-} = \frac{\sqrt{V_0 - \beta_N^{m_1}} + W_N^{m_1}(\eta, -\Delta, x_0)}{\sqrt{V_0 - \beta_N^{m_1}} - W_N^{m_1}(\eta, -\Delta, x_0)} \times \exp[-2\sqrt{V_0 - \beta_N^{m_1}} x_0].$$

In Fig. 4, we show two exact surface states for $\eta = 0.3$, $\Delta = 0.1$ and $N = 0$. The surface waves strongly depend

on the two interface positions. For $x_0 = -\pi/2$ and $x_1 = \pi$ [or $x_0 = -7\pi/6$ and $x_1 = \pi/2$], the surface state has an asymmetric distribution, see Fig. 4(a) [or (b)]. While for $x_0 = -\pi/2$ and $x_1 = \pi/2$, it becomes symmetric, see Fig. 4(c).

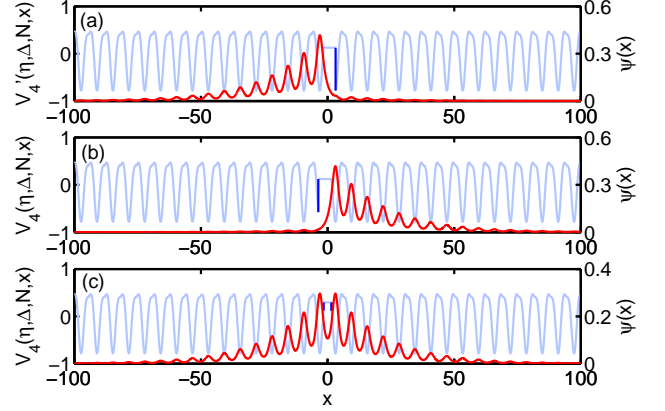


FIG. 4: (Color online). Exact surface states in a double-interface system described by $V_4(\eta, \Delta, N, x)$ with $\eta = 0.3$, $\Delta = 0.1$ and $N = 0$. (a) $x_0 = -\pi/2$, $x_1 = \pi$, $V_0 = 0.13$, and $R = 0.0255412$. (b) $x_0 = -7\pi/6$, $x_1 = \pi/2$, $V_0 = 0.120845$, and $R = 254.28$. (c) $x_0 = -x_1 = -\pi/2$, $V_0 = 0.30$, and $R = 1.0$.

V. CONCLUSION

In conclusion, by using the superpositions of finite numbers of unstable Bloch states for the corresponding infinite periodic systems, we have given an analytical approach for constructing exact surface states in photonic superlattices. These exact surface states have the same propagation constants for the finite-superposition states in the energy gaps and so that they are a kind of stable in-gap states. This analytical method has been used to find the exact surface states in several typical systems involving a single or two interfaces. By matching two solutions (a finite-superposition solution and a free-space solution or two finite-superposition solutions) at two sides of the interfaces, the existence conditions for surface states are obtained analytically from the continuity conditions. The existence and the shapes of the exact surface states not only depend on the interface parameters, but also rely on the lattice parameters. Our results give an analytical demonstration of the existence of the surface states and should shine light on understanding and controlling the surface waves.

Acknowledgments

The authors acknowledge Yuri S. Kivshar for his valuable comments. This work is supported by the NBRPC

under Grant No. 2012CB821300 (2012CB821305), the NNSFC under Grants No. 10905019 and No. 11075223, the PCSIRT under Grant No. IRT0964, the NCETPC

under Grant No. NCET-10-0850, the Construct Program of the National Key Discipline and the Fundamental Research Funds for Central Universities of China.

-
- [1] I. E. Tamm, Phys. Z. Sowjetunion 1, 733 (1932).
 [2] W. Shockley, Phys. Rev. 56, 317 (1939).
 [3] H. Ohno, E.E. Mendez, J.A. Brum, J.M. Hong, F. Agulló-Rueda, L.L. Chang, and L. Esaki, Phys. Rev. Lett. 64, 2555 (1990).
 [4] T. Miller and T.-C. Chiang, Phys. Rev. Lett. 68, 3339 (1992).
 [5] M. Zahler, E. Cohen, J. Salzman, E. Linder and L.N. Pfeiffer, Phys. Rev. Lett. 71, 420 (1993).
 [6] M. Zahler, E. Cohen, J. Salzman, E. Linder, E. Maayan and L.N. Pfeiffer, Phys. Rev. B 50, 5305 (1994).
 [7] A.B. Henriques, L.K. Hanamoto, P.L. Souza, and B. Yavich, Phys. Rev. B 61, R13369 (2000).
 [8] P. Yeh, A. Yariv, and A.Y. Cho, Appl. Phys. Lett. 32, 104 (1978).
 [9] N. Malkova, I. Hromada, X. Wang, G. Bryant, and Z. Chen, Opt. Lett. 34,1633 (2009).
 [10] N. Malkova, I. Hromada, X. Wang, G. Bryant, and Z. Chen, Phys. Rev. A 80, 043806 (2009).
 [11] A.V. Kavokin, I. A. Shelykh, and G. Malpuech, Phys. Rev. B 72, 233102 (2005).
 [12] T. Goto, A.V. Dorofeenko, A.M. Merzlikin, A.V. Baryshev, A.P. Vinogradov, M. Inoue, A.A. Lisyansky, and A.B. Granovsky, Phys. Rev. Lett. 101, 113902 (2008).
 [13] T. Goto, A.V. Baryshev, M. Inoue, A.V. Dorofeenko, A.M. Merzlikin, A.P. Vinogradov, A.A. Lisyansky, and A.B. Granovsky, Phys. Rev. B 79, 125103 (2009).
 [14] A.B. Khanikaev, A.V. Baryshev, M. Inoue, and Y. S. Kivshar, Appl. Phys. Lett. 95, 011101 (2009).
 [15] V. Heine, Surface Sci. 2, 1 (1964); Phys. Rev. 138, A1689 (1965).
 [16] F. Forstmann and V. Heine, Phys. Rev. Lett. 24, 1419(1970).
 [17] J. D. Levine, Phys. Rev. 171, 701 (1968).
 [18] M. Steslicka, R. Kucharczyk, and M. L. Glasser, Phys. Rev. B 42, 1458 (1990).
 [19] J. D. Levine and P. Mark, Phys. Rev. 182, 926 (1969).
 [20] R.H. Yu, Phys. Rev. B 47, 15 692 (1993).
 [21] H.K. Sy and T.C. Chua, Phys. Rev. B 48, 7930 (1993).
 [22] N. Malkova and C.Z. Ning, Phys. Rev. B 73, 113113 (2006).
 [23] N. Malkova and C.Z. Ning, Phys. Rev. B 76, 045305 (2007).
 [24] A.P. Vinogradov, A.V. Dorofeenko, S.G. Erokhin, M. Inoue, A.A. Lisyansky, A.M. Merzlikin, and A.B. Granovsky, Phys. Rev. B 74, 045128 (2006).
 [25] G. Lenz and J. Salzman, Appl. Phys. Lett. 56, 871 (1990).
 [26] G. Ihm, S.K. Noh, M.L. Falk and K.Y. Lim, J. Appl. Phys. 72, 5325 (1992).
 [27] G. Della Valle, M. Ornigotti, E. Cianci, V. Foglietti, P. Laporta, and S. Longhi, Phys. Rev. Lett. 98, 263601 (2007).
 [28] K. Shandarova et al., Phys. Rev. Lett. 102, 123905 (2009).

Appendix: Derivation of the Bloch-wave solutions

$$\psi_N^{m_1}(\eta, \Delta, x)$$

Below, we give more details about how to derive the Bloch-wave solutions

$$\begin{aligned} \psi_N^{m_1}(\eta, \Delta, x) = & \exp \left[- \left(\frac{\Delta}{2} x + 2\eta \cos x \right) \right] \\ & \times \sum_{n=0}^N \left[a_n \cos \left(\frac{N}{2} - n \right) x - b_n \sin \left(\frac{N}{2} - n \right) x \right], \end{aligned} \quad (\text{A.1})$$

for the Schrödinger equation

$$- \frac{d^2}{dx^2} \psi(x) + V(x)\psi(x) = \beta \psi(x), \quad (\text{A.2})$$

with

$$\begin{aligned} V(x) = & -n'_1 \cos(2x) + n'_2 \cos(x + \theta) \\ = & -n'_1 \cos(2x) + n'_2 \cos \theta \cos x - n'_2 \sin \theta \sin x. \end{aligned}$$

By applying the transformations

$$\xi = \exp[-ix], \quad (\text{A.3})$$

$$\psi(x) = \exp[-\sqrt{2n'_1} \cos x] \xi^\lambda \phi(\xi), \quad (\text{A.4})$$

with

$$\lambda = \frac{\sqrt{2n'_1} - n'_2 \cos \theta - in'_2 \sin \theta}{2\sqrt{2n'_1}},$$

we have

$$\begin{aligned} \xi^2 \frac{d^2 \phi}{d\xi^2} + \left[\sqrt{2n'_1} - \sqrt{2n'_1} \xi^2 + (2\lambda + 1)\xi \right] \frac{d\phi}{d\xi} \\ + \left[\lambda^2 - \beta - n'_1 - \left(\sqrt{2n'_1} - n'_2 \cos \theta \right) \xi \right] \phi = 0. \end{aligned} \quad (\text{A.5})$$

By writing the solution in form of a standard power-series expansion

$$\phi(\xi) = \sum_{n=0}^{\infty} d_n \xi^n \quad (\text{A.6})$$

from Eq. (A.5), one can easily find that the coefficients d_n are determined by a three-term recurrence relation

$$\begin{aligned} \sqrt{2n'_1}(n+2)d_{n+2} + \left[n'_2 \cos \theta - \sqrt{2n'_1}(n+1) \right] d_n \\ + \left[(n+1)(n+2\lambda+1) + \lambda^2 - n'_1 - \beta \right] d_{n+1} = 0, \end{aligned} \quad (\text{A.7})$$

with the initial condition $d_0 = 1$ and $d_{-1} = 0$. From this three-term recurrence relation, we obtain a necessary condition

$$n'_2 \cos \theta = \sqrt{2n'_1}(N+1), \quad (\text{A.8})$$

$$d_{N+1} = 0, \quad (\text{A.9})$$

with non-negative integers $N = (0, 1, 2, \dots)$. Therefore, the series solution $\phi(\xi)$ can be terminated as a polynomial of degree N for ξ . The coefficient d_{N+1} is a polynomial of degree $N+1$ in β . If β is a real root of this polynomial, we have a truncated series solution $\phi_N(\xi)$. We thus have

$$\begin{aligned} \psi(x) = & \exp \left[i \left(\frac{N}{2} + i \frac{n'_2 \sin \theta}{2\sqrt{2n'_1}} \right) x - \sqrt{2n'_1} \cos x \right] \\ & \times \sum_{n=0}^N d_n \exp[-inx]. \end{aligned} \quad (\text{A.10})$$

It is clearly seen that $\psi(x)$ represent Bloch-wave solutions

with the wave vector $k = N/2 + i \frac{n'_2 \sin \theta}{2\sqrt{2n'_1}}$. If we take $\sqrt{2n'_1} = 2\eta$, $n'_2 \cos \theta = 2\eta(N+1)$ and $n'_2 \sin \theta = 2\eta\Delta$, we have $n'_1 = 2\eta^2$, $n'_2 = 2\eta\sqrt{(N+1)^2 + \Delta^2}$, and $\theta = \arctan(\Delta/(N+1))$.

Due to $V(x)$ is a real function, we can take the real part of $\psi(x)$ as a solution of Eq. (A.2)

$$\begin{aligned} \psi_N^{m_1}(\eta, \Delta, x) = & \exp \left[- \left(\frac{\Delta}{2} x + 2\eta \cos x \right) \right] \\ & \times \sum_{n=0}^N \left[a_n \cos \left(\frac{N}{2} - n \right) x - b_n \sin \left(\frac{N}{2} - n \right) x \right], \end{aligned} \quad (\text{A.11})$$

where $d_n = a_n + ib_n$, and the index m_1 corresponds to the m_1 -th real zero of $d_{N+1}(\eta, \Delta, \beta) = a_{N+1} + ib_{N+1} = 0$ in ascending order. This completes the derivation of Bloch-wave solutions (A.1).